

## Supporting Information

### **Hybrid Engineering of crystalline NiSe<sub>x</sub> nanorod arrays with amorphous Ni-P film towards promoted overall water electrocatalysis**

Xiaohu Xu <sup>a\*</sup>, Le Su <sup>a</sup>, Yujie Zhang <sup>a</sup>, Lijuan Dong <sup>b\*</sup>, Xiangyang Miao <sup>a\*</sup>

<sup>a</sup> Key Laboratory of Spectral Measurement and Analysis of Shanxi Province,  
College of Physics and Information Engineering, Shanxi Normal University, No.339  
Taiyu road, Xiaodian District, Taiyuan 030031, China

<sup>b</sup> Shanxi Provincial Key Laboratory of Microstructure Electromagnetic Functional  
Materials, Shanxi Datong University, Xingyun street, Nanjiao District, Datong,  
037009, China.

\*Corresponding author. E-mail: bigbrowm@163.com; Tel:+86-13623578753

\*Corresponding author. E-mail: donglijuan\_2012@163.com; Tel:+86-13994319080

\*Corresponding author. E-mail: sxxymiao@126.com; Tel:+86-15035757788

Number of pages: 16

Number of figures: 15

Number of tables: 3

**Content**

## Experimental Section

HRTEM images.....	Fig. S1
EDX plot.....	Fig. S2
Raman spectrum.....	Fig. S3
Contact angle measurement.....	Fig. S4
LSV curves with different deposition potential.....	Fig. S5
LSV curves with different deposition time.....	Fig. S6
LSV curves with different amounts of $\text{NaH}_2\text{PO}_2$ .....	Fig. S7
Quantitative $\text{H}_2$ measurement .....	Fig. S8
Cyclic voltammograms with different scanning rate.....	Fig. S9
SEM images after stability test for HER .....	Fig. S10
EDX plot after stability test for HER.....	Fig. S11
XPS spectra after stability test for HER.....	Fig. S12
SEM images after stability test for OER.....	Fig. S13
EDX plot after stability test for OER.....	Fig. S14
XPS spectra after stability test for OER.....	Fig. S15
Comparison of HER performance.....	Table S1

Comparison of OER performance.....Table S2

Comparison of Cell voltage.....Table S3

### **Materials**

All chemicals were of analytical grade and used without further purification in the experiments. Hydrochloric acid (HCl), potassium hydroxide (KOH), anhydrous ethanol, acetone, Se powders, sodium borohydride (NaBH<sub>4</sub>), sodium hypophosphite (NaH<sub>2</sub>PO<sub>2</sub>) and nickel nitrate hexahydrate (Ni(NO<sub>3</sub>)<sub>2</sub>·6H<sub>2</sub>O) were purchased from Sinopharm Chemical Reagent Co., Ltd. Nickel foam (NF) was obtained from the KunShan Kunag Xun Electronics Co., Ltd. Pt/C (20 wt % Pt), ruthenium(IV) oxide (RuO<sub>2</sub>) and Nafion (5 wt %) were purchased from Aladdin Ltd. The deionized (DI) water used in all experiments with a resistivity of 18.2 MΩ·cm<sup>-1</sup> was purified through a Millipore system.

### **Characterization**

X-ray diffraction (XRD) patterns were obtained by X-ray diffractometer (Bruker D8-Advance) equipped with a Cu K $\alpha$  radiation source ( $\lambda = 1.5418 \text{ \AA}$ ) to record the crystal diffraction patterns of samples. The morphology and structure of all samples were characterized by field-emission scanning electron microscopy (FE-SEM, Hitachi, SU-8010) and high-resolution transmission electron microscopy (HR-TEM, JEM-2100, 200 kV) with X-ray energy-dispersive spectroscopy. The surface composition and valence state of the samples were characterized by X-ray photoelectron spectroscopy (XPS, Kratos Axis Ultra DLD). Raman characterization was performed

on a Renishaw-inVia Raman spectrometer with 532 nm laser excitation. The static contact angle is measured by JY-82B Kruss DSA system at room temperature.

### **Electrochemical measurements**

All electrochemical data tests were achieved by CHI 760E electrochemical workstation (CH Instruments, China) with a three-electrode system in an O<sub>2</sub> saturated 1.0 M KOH. The as-prepared samples supported on Ni foam, a mercury oxide electrode (Hg/HgO) and a carbon rod (4 mm in diameter) were employed as the working, reference and counter electrode, respectively. Cyclic Voltammetry (CV) measurements for OER and HER were scanned in the potential range from 0 to 1 V (vs. Hg/HgO), -1.5 to -1 V (vs. Hg/HgO) at a scanning rate of 200 mV·s<sup>-1</sup>, respectively. And the corresponding polarization curves were obtained by using Linear Sweep Voltammetry (LSV) with a scan rate of 3 and 5 mV·s<sup>-1</sup>, respectively. The stability test was implemented using chronopotentiometric method at certain potentials. In addition, the polarization curve of the OWS was measured from 1.0 to 2.0 V at a sweep rate of 5 mV s<sup>-1</sup> via a two-electrode configuration in 1 M KOH, and the chronopotentiometric curve was recorded at a constant potential of 1.52 V. The electrochemical data were not collected until the signals of working electrodes stabilized after scanning several times. Electrochemical impedance spectroscopy (EIS) experiments were conducted in the frequency range from 100 KHz to 1 Hz with an amplitude potential of 5 mV. All the potentials with regard to Hg/HgO were calibrated to the reversible hydrogen electrode (RHE) according to the following equation:  $E(\text{RHE}) = E(\text{vs. Hg/HgO}) + 0.059 \times \text{pH} + 0.098$ . All the measurements

above were corrected by manual iR compensation using the current and the solution resistance. Furthermore, all experiments were repeated at least three times to ensure reliability and reproducibility.

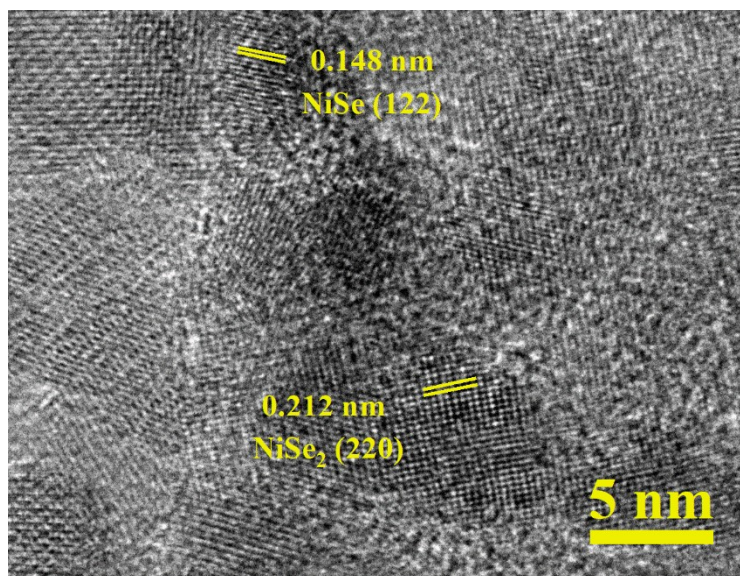


**Fig. S1.** HRTEM images of Ni-P/NiSe<sub>x</sub>.

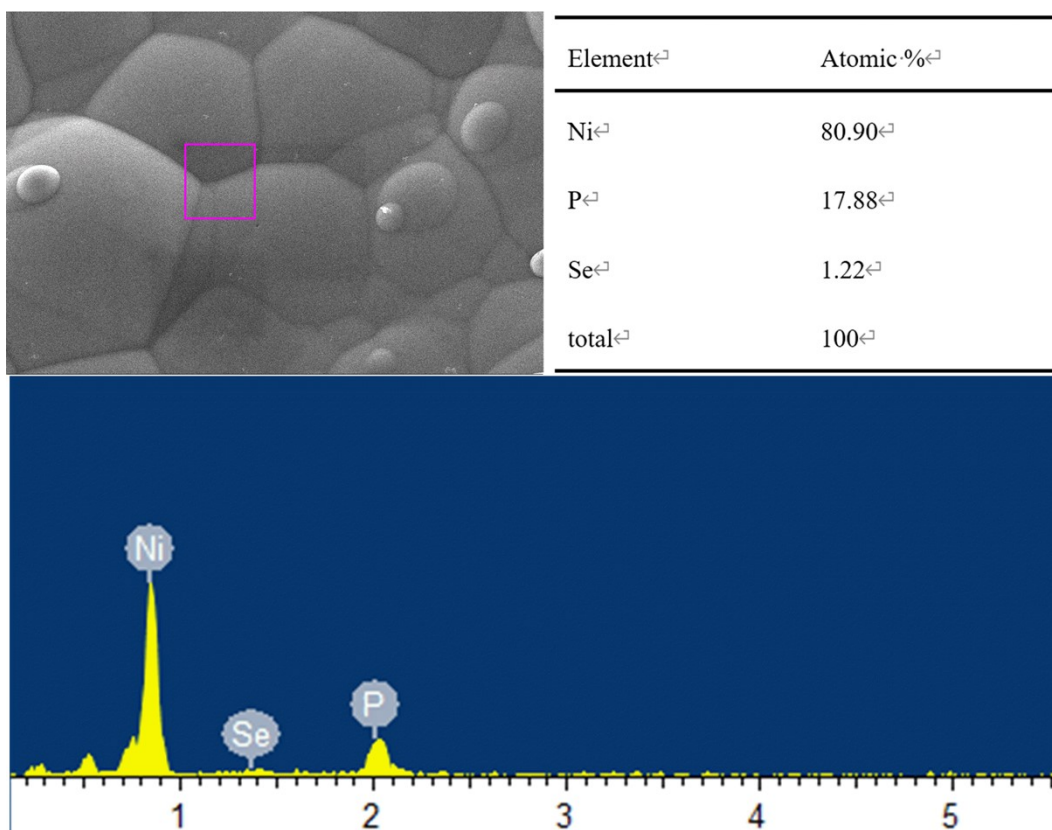


**Fig. S2.** Corresponding EDX plot of the Ni-P/NiSe<sub>x</sub>/NF catalyst.

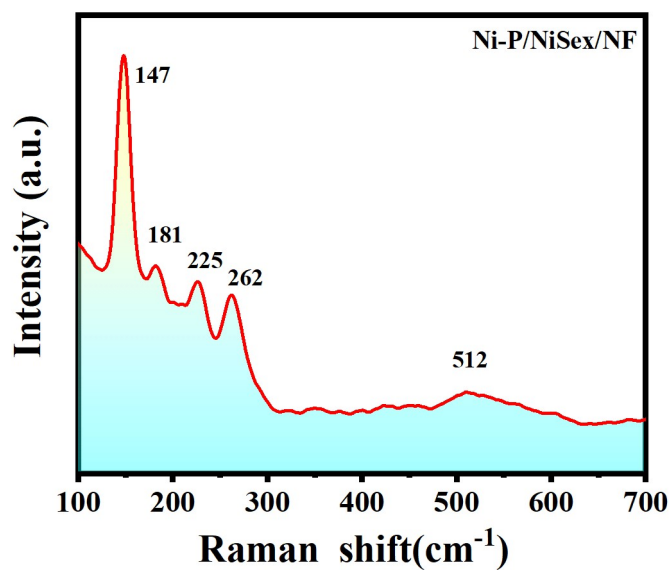


Fig. S3. Raman spectrum of as-prepared Ni-P/NiSe<sub>x</sub>/NF.

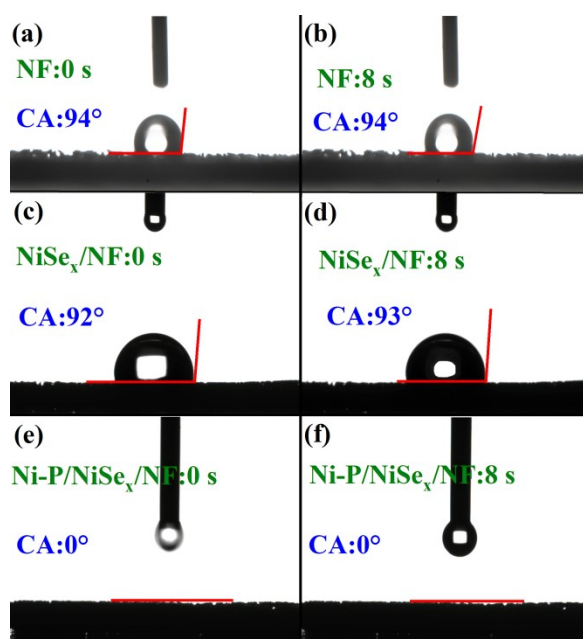
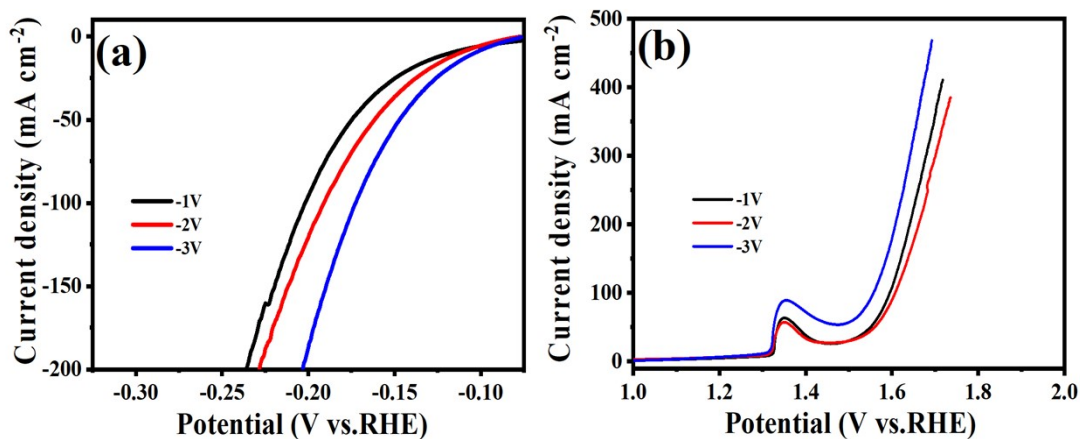
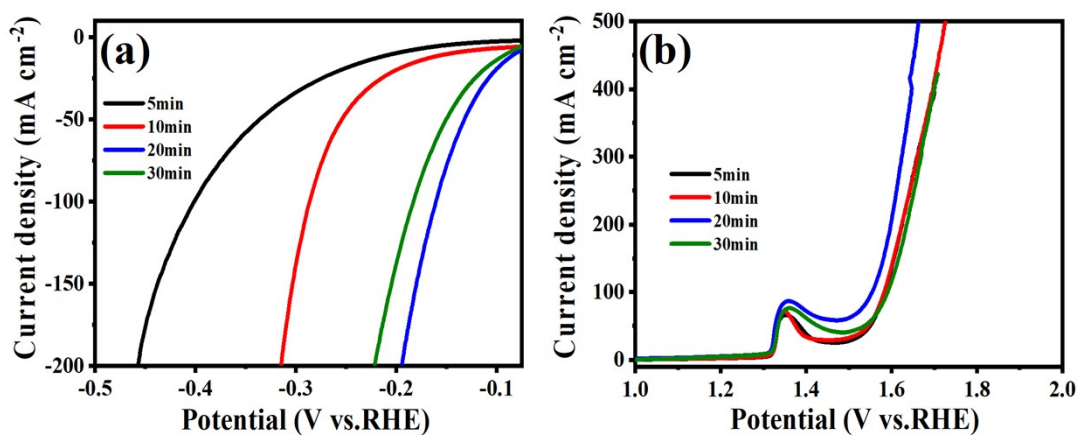


Fig. S4. Contact angle measurement of samples NF (a, b), NiSe<sub>x</sub>/NF (c, d) and Ni-P/NiSe<sub>x</sub>/NF (e, f) catalysts at 0 and 8 s standing time (using a drop of 1.0 M KOH solution).



**Fig. S5.** (a) HER and (b) OER polarization curves of Ni-P/NiSe<sub>x</sub>/NF synthesized with different deposition potential (-1, -2, -3 V).



**Fig. S6.** (a) HER and (b) OER polarization curves of Ni-P/NiSe<sub>x</sub>/NF synthesized with different deposition time (5, 10, 20, 30 min).

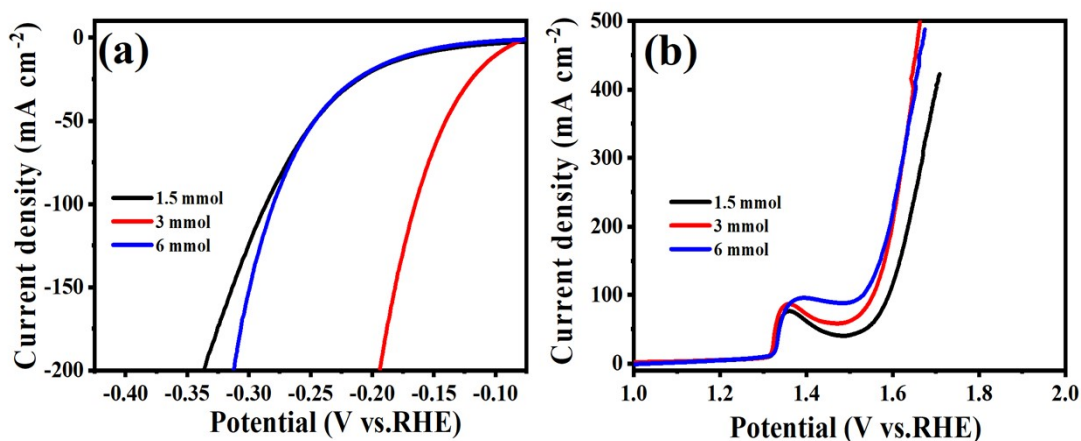


**Fig. S7.** (a) HER and (b) OER polarization curves of Ni-P/NiSe<sub>x</sub>/NF samples synthesized with different amounts of NaH<sub>2</sub>PO<sub>2</sub> (1.5, 3, 6 mmol).

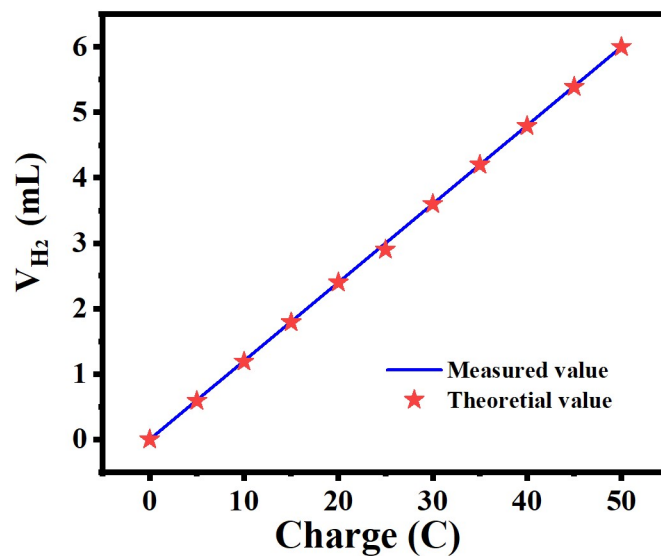


Fig. S8. Quantitative  $H_2$  measurement via water displacement.

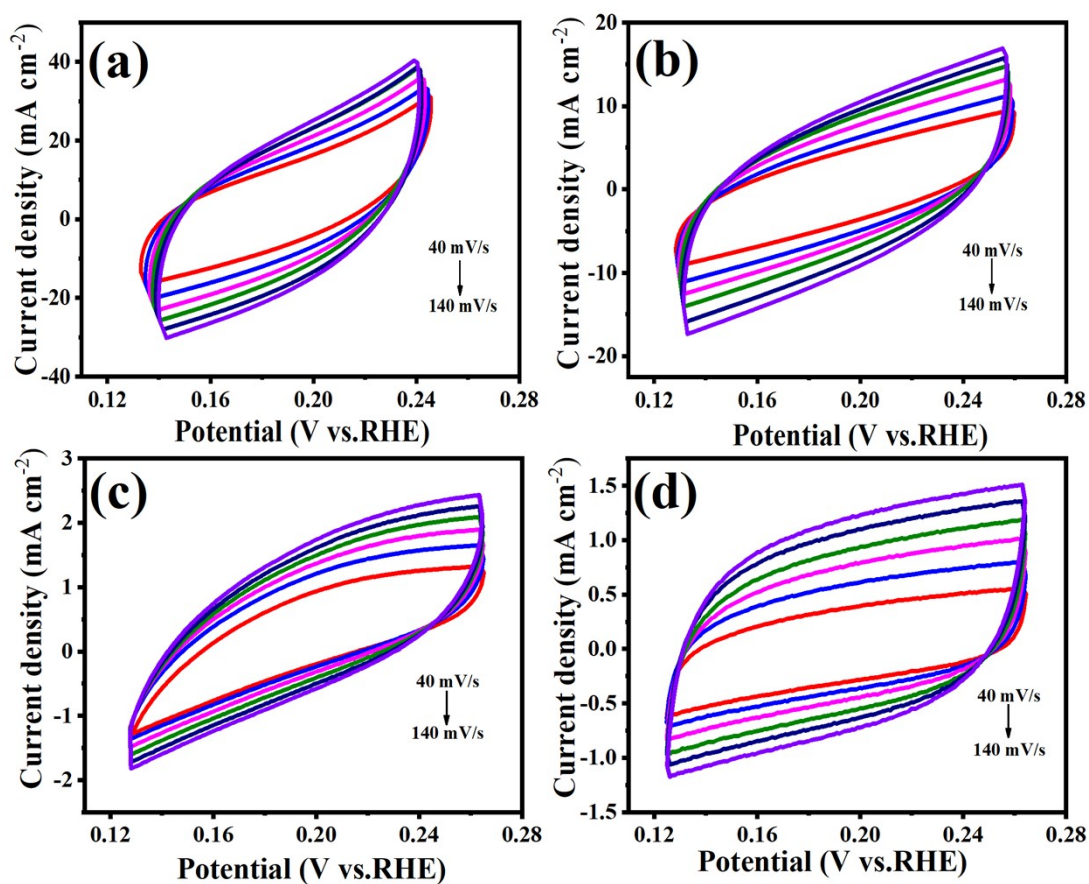
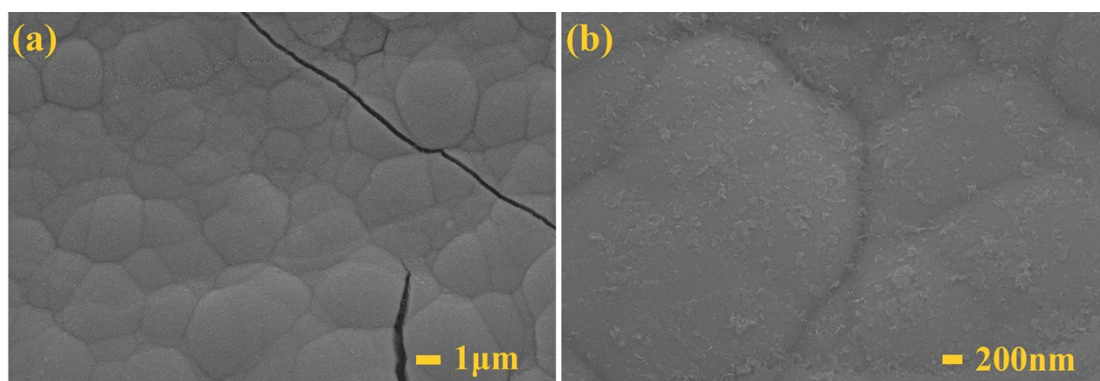
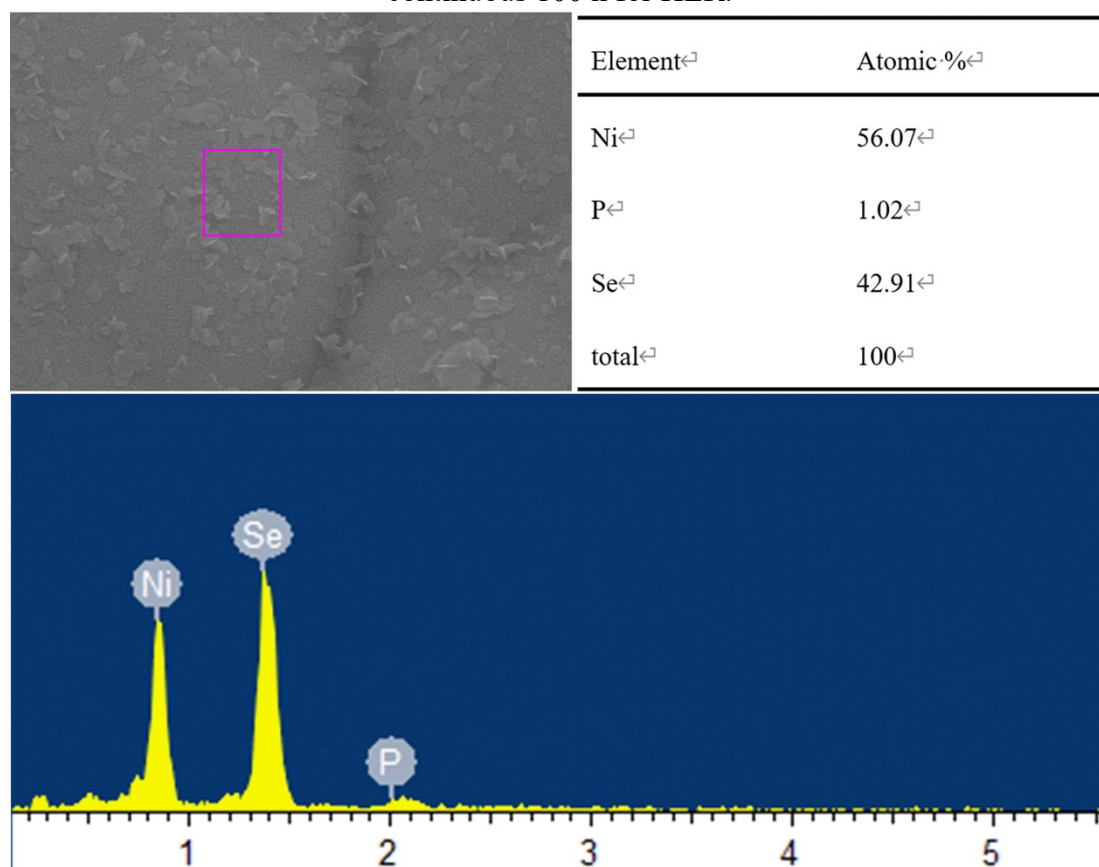


Fig. S9. CV curves of (a) Ni-P/NiSe<sub>x</sub>/NF, (b) Ni-P/NF, (c) NiSe<sub>x</sub>/NF, (d) NF in the non-faradaic region with different scanning rates from 40 to 140 mV·s<sup>-1</sup>.





**Fig. S10.** Representative SEM images of the Ni-P/NiSe<sub>x</sub>/NF catalyst after continuous 100 h for HER.



**Fig. S11.** Corresponding EDX plot of the Ni-P/NiSe<sub>x</sub>/NF catalyst after continuous 100 h for HER.

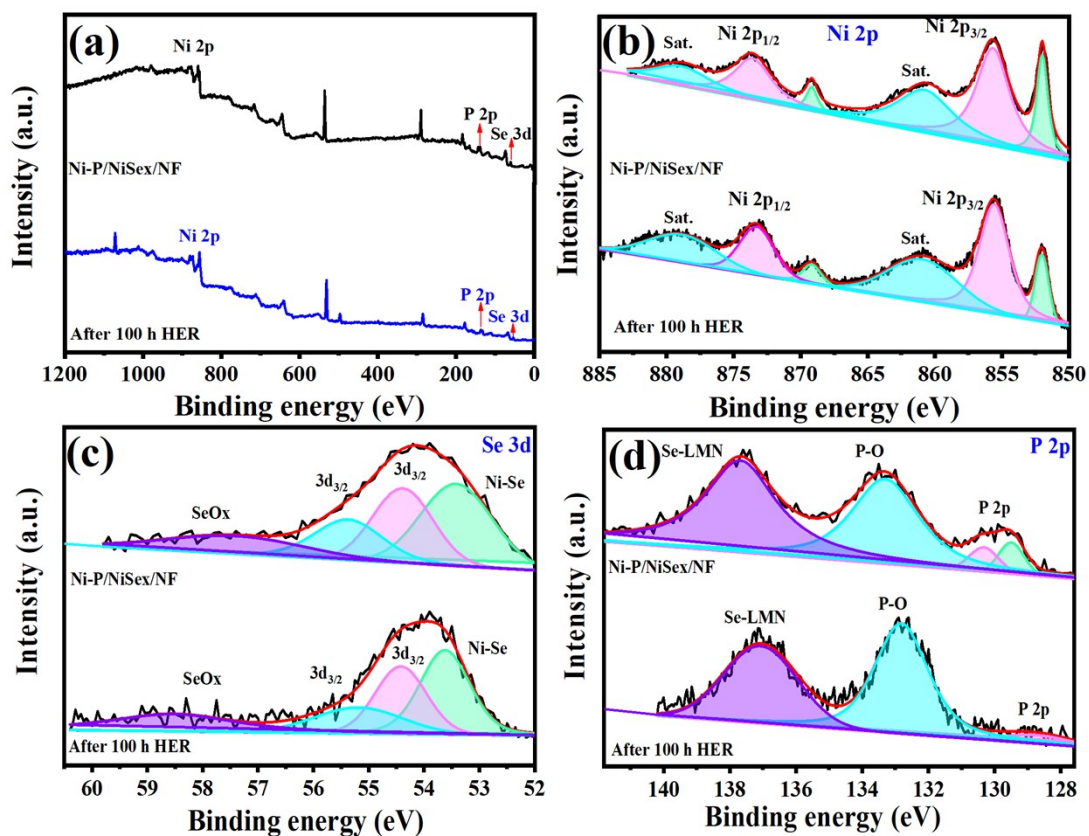


**Fig. S12.** (a) XPS full survey spectrum of Ni-P/NiSe<sub>x</sub>/NF after HER electrolysis. High-resolution XPS spectrum: (b) Ni 2p, (c) Se 3d, and (d) P 2p.

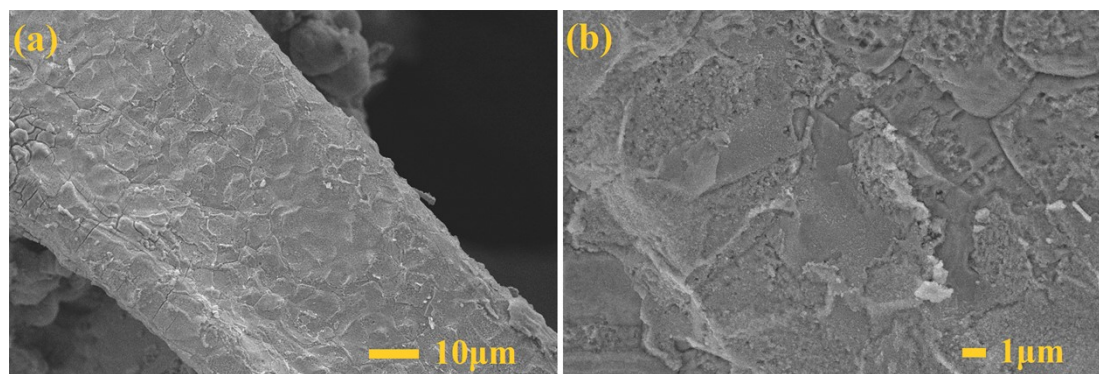


**Fig. S13.** Representative SEM images of the Ni-P/NiSe<sub>x</sub>/NF catalyst after continuous 100 h for OER.

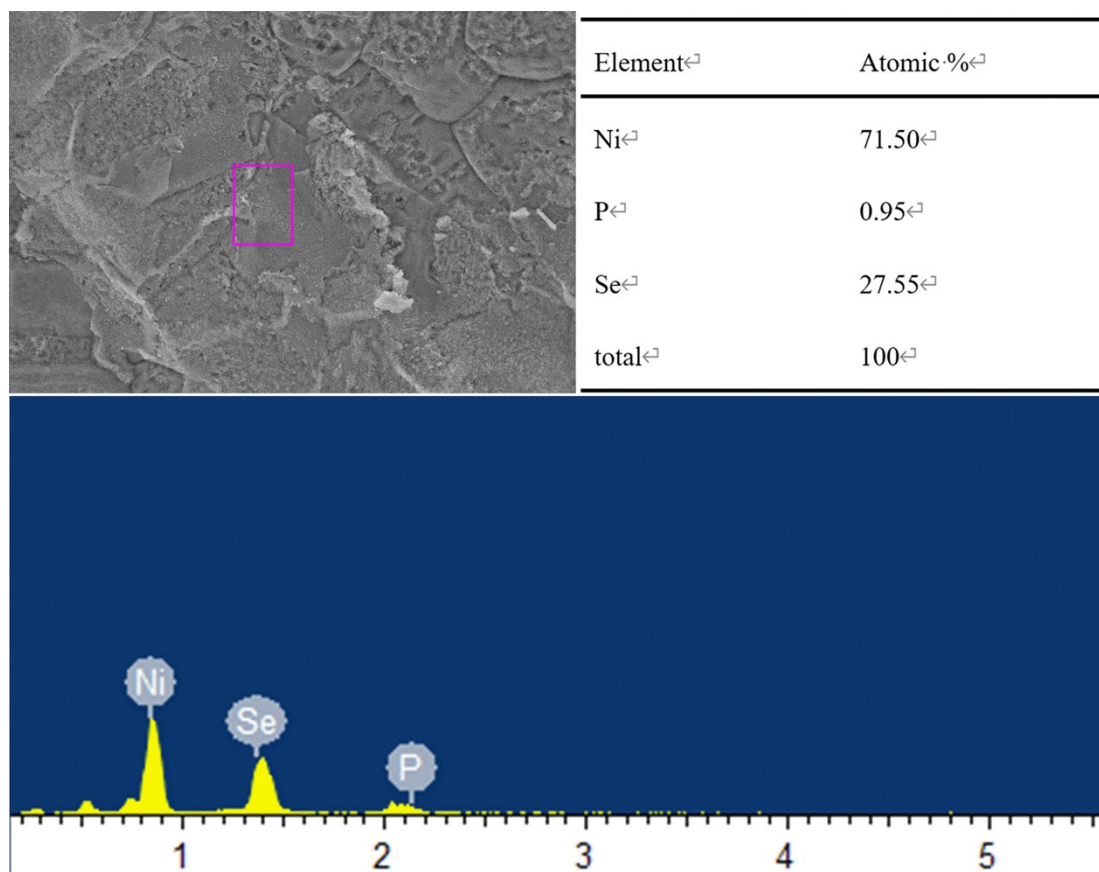


**Fig. S14.** Corresponding EDX plot of the Ni-P/NiSe<sub>x</sub>/NF catalyst after continuous 100 h for OER.

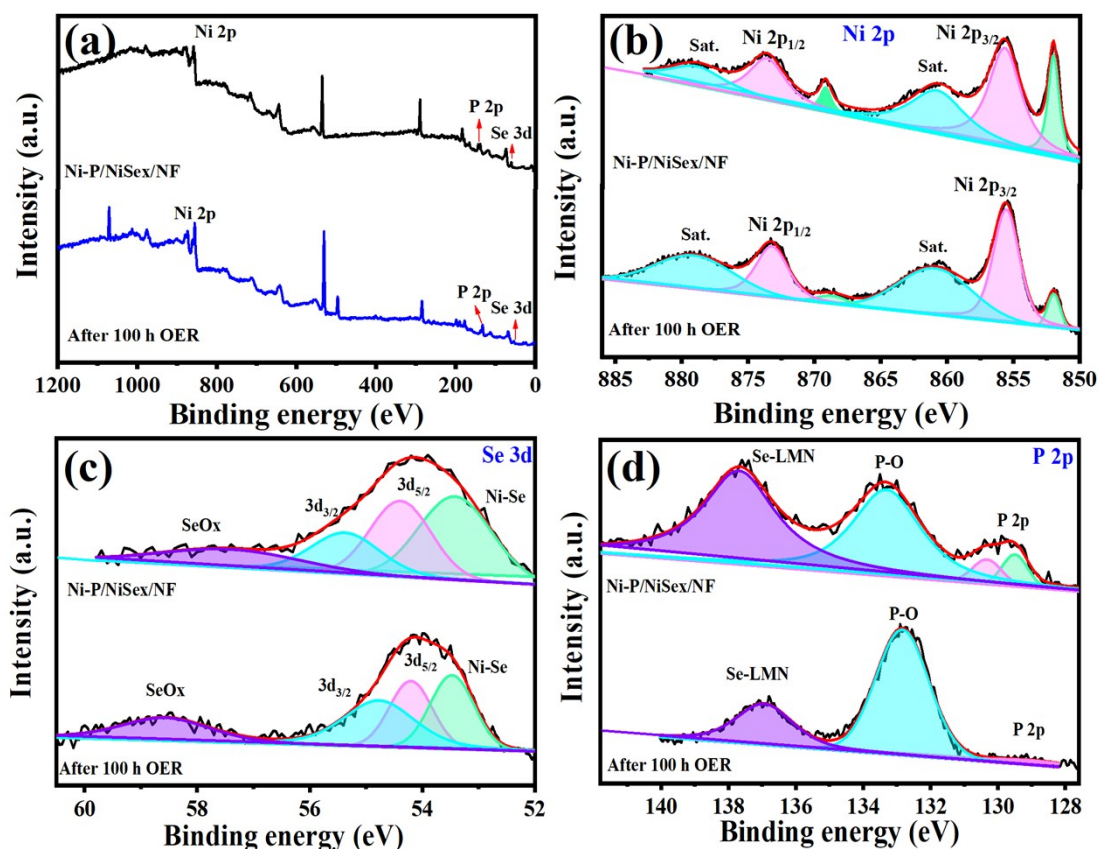


**Fig. S15.** (a) XPS full survey spectrum of Ni-P/NiSe<sub>x</sub>/NF after OER test. High-resolution XPS spectrum: (b) Ni 2p, (c) Se 3d, and (d) P 2p.

**Table. S1.** Comparisons of HER catalytic activity of Ni-P/NiSe<sub>x</sub>/NF with some previous reported catalysts in 1 mol/L KOH solution.

Material	Substrate	Overpotential	Overpotential	Reference
		HER@ 10mAcm <sup>-2</sup>	HER@ 100mA cm <sup>-2</sup>	
Ni-P/NiSe <sub>x</sub>	Ni foam	98	165	This work
Co <sub>0.85</sub> Se P	Graphene	150	180 @20mAcm <sup>-2</sup>	Adv. Mater 2017, 29,1701589 <sup>1</sup>
Ni <sub>3</sub> Se <sub>2</sub>	Ni foam	203	279	Nano Energy 2016, 24,103 <sup>2</sup>
MoSe <sub>2</sub> @Ni <sub>0.85</sub> Se	Ni foam	117	204	Electrochim. Acta 2017, 712 <sup>3</sup>
NiSe <sub>2</sub> @NiO <sub>x</sub>	Glassy	132	-	

	carbon			Small 2017, 13, 1701487 <sup>4</sup>
<b>Fe,Co-NiSe<sub>2</sub></b>	carbon fiber cloth	92	245 @200mAc <sup>m</sup> - <sup>2</sup>	Adv. Mater. 2018, 30, 1802121 <sup>5</sup>
<b>NiSe</b>	Ni foam	177	-	Adv. Energy Mater. 2018, 8, 1702704 <sup>6</sup>
<b>NiSe</b>	Ni foam	96	270 @20mAc <sup>m</sup> - <sup>2</sup>	Angew. Chem. Int. Edit. 2015,54, 9351 <sup>7</sup>
<b>Ni<sub>2</sub>P</b>	Glassy carbon	220	290	Energy Environ. Sci 2015,8, 2347 <sup>8</sup>
<b>Ni/Ni<sub>8</sub>P<sub>3</sub></b>	Ni foam	130	270 @30mAc <sup>m</sup> - <sup>2</sup>	Adv. Funct. Mater. 2016, 26,3314 <sup>9</sup>
<b>NiSe-Ni<sub>0.85</sub>Se</b>	Carbon Paper	101	131	Small 2018, 14, 1800763 <sup>10</sup>
<b>CP@Ni-P</b>	Carbon Fiber Paper	117	250	Adv. Funct. Mater. 2016, 26, 4067 <sup>11</sup>
<b>Ni<sub>90</sub>P<sub>10</sub></b>	Ti plate	234	-	Chem. Commun. 2018, 54, 12408 <sup>12</sup>
<b>O<sub>3</sub>-V<sub>10</sub>-Ni<sub>2</sub>P</b>	Glassy carbon	108	-	Nano Energy 2018,54,82 <sup>13</sup>
<b>EG/Ni<sub>3</sub>Se<sub>2</sub> /Co<sub>9</sub>S<sub>8</sub></b>	graphene foil	170 @20mAc <sup>m</sup> - <sup>2</sup>	230 @50mAc <sup>m</sup> - <sup>2</sup>	Nano Lett. 2017, 17, 4202 <sup>14</sup>
<b>o-CoSe<sub>2</sub> P</b>	Glassy carbon	104	-	Nat. Commun. 2018, 9, 2533 <sup>15</sup>
<b>NixCo<sub>3-x</sub>S<sub>4</sub>/ Ni<sub>3</sub>S<sub>2</sub></b>	Ni foam	136	258	Nano Energy 2017,35,161 <sup>16</sup>
<b>Mo<sub>2</sub>C</b>	Ni foam	130	215	Electrochim. Acta 2019,298, 305 <sup>17</sup>

<b>Co<sub>0.9</sub>Fe<sub>0.1</sub>-Se</b>	Ni foam	125	229	J. Energy Chem. 2021,60,194-201 <sup>18</sup>
<b>NiSe/RGO</b>	Ni mesh	102	-	J. Mater. Chem. A 2016,4,14789 <sup>19</sup>
<b>NiSe<sub>2</sub></b>	Ti foam	100	-	Nanoscale 2016,8,3911-3915 <sup>20</sup>
<b>NiSe<sub>2</sub> nanoparticles</b>	Glassy carbon	190	-	ACS Appl. Mater. Inter. 2016,8,5327-5334 <sup>21</sup>
<b>Fe<sub>7.4%</sub>-NiSe</b>	Ni foam	163	265	J. Mater. Chem. A 2019,7,2233-2241 <sup>22</sup>

**Table. S2.** Comparison of OER catalytic performance of Ni-P/NiSe<sub>x</sub>/NF with other recently reported non-precious metal electrocatalysts in 1 mol/L KOH solution.

<b>Catalyst</b>	<b>Substrate</b>	<b>Overpotential (mV) @ 100 mA·cm<sup>-2</sup></b>	<b>Reference</b>
<b>Ni-P/NiSe<sub>x</sub></b>	Ni foam	320	This work
<b>Co<sub>0.9</sub>Fe<sub>0.1</sub>-Se</b>	Ni foam	287	J. Energy Chem. 2021,60,194-201
<b>Co<sub>2</sub>P/CoNPC</b>	Glassy carbon	326@10	Adv. Mater. 2020,32,2003649.
<b>O-CoP</b>	Glassy carbon	310@10	Adv. Funct. Mater. 2020,30,1905252.
<b>NiSe<sub>2</sub></b>	Ti foam	295@20	ACS Appl. Mater. Inter. 2016,8,4718
<b>Co-NiSe</b>	Ni foam	330@50	ACS Sustainable Chem. Eng. 2019,7,19257-19267
<b>Co<sub>9</sub>S<sub>8</sub>@NiCo-LDH</b>	Ni foam	330	Sci. Bull. 2019,64(3),158-165
<b>Co<sub>0.13</sub>Ni<sub>0.87</sub>Se<sub>2</sub></b>	Ti foam	320	Nanoscale 2016;8:3911-3915

<b>P-NiS<sub>2</sub>-500</b>	Ni foam	350	Chem. Eng. J. 2021,420,127630
<b>Ni<sub>3</sub>Se<sub>2</sub> nanoforest</b>	Ni foam	353	Nano Energy, 2016,24,103-110
<b>NiSe nanowire film</b>	Ni foam	270@20	Angew. Chem. Int. Ed. 2015,54,9351-9355
<b>Ni<sub>x</sub>P<sub>y</sub></b>	Carbon fiber paper	320@10	ACS Appl. Mater. Inter. 2016,8,10826-10834
<b>NiP</b>	Ni foam	350@50	J. Energy Chem. 2017,26,1196-1202

**Table S3.** Comparison cell voltage of hierarchical Ni-P/NiSe<sub>x</sub>/NF with other bifunctional electrocatalysts in 1 mol/L KOH solution.

<b>Catalyst</b>	<b>Substrate</b>	<b>cell voltage (V) @ j=10 mA·cm<sup>-2</sup></b>	<b>Reference</b>
<b>Ni-P/NiSe<sub>x</sub></b>	Ni foam	1.536	This work
<b>NiSe-Ni<sub>0.85</sub>Se</b>	Carbon fiber paper	1.62	Small 2018,14,1800763
<b>Co<sub>0.85</sub>Se/FeNi-LDH</b>	Graphene foil	1.67	Energ. Environ. Sci., 2016,9(2),478-483
<b>NiCo<sub>2</sub>S<sub>4</sub>/NiFe-LDH</b>	Ni foam	1.60	ACS Appl. Mater. Inter. 2017,9(18),15364-15372
<b>Co<sub>0.9</sub>Fe<sub>0.1</sub>-Se</b>	Ni foam	1.55	J. Energy Chem. 2021,60,194-201
<b>Co<sub>3</sub>S<sub>4</sub>@NiCo-LDH</b>	Ni foam	1.59	New J. Chem. 2021,45,15429
<b>Co<sub>0.75</sub>Ni<sub>0.25</sub>Se</b>	Ni foam	1.60	Nanoscale 2019,11,7959-7966
<b>NiCoSe<sub>2</sub></b>	Carbon cloth	1.62	J. Mater. Chem. A 2018,6,17353-17360
<b>Ni<sub>8</sub>P<sub>3</sub></b>	Ni foam	1.61	J. Am. Chem. Soc. 2016,26,3314-3323
<b>Ni<sub>2</sub>P</b>	Glassy carbon	1.63	Energy Environ. Sci. 2015,8,2347-2351
<b>NiP</b>	Ni foam	1.63	J. Energy Chem. 2017,26,1196-1202
<b>Porous Co<sub>0.75</sub>Ni<sub>0.25</sub>(OH)<sub>2</sub> nanosheets</b>	Carbon fiber paper	1.56	Small 2019,15,1804832

## References

1. Hou, Y.; Qiu, M.; Zhang, T.; Zhuang, X.; Kim, C. S.; Yuan, C.; Feng, X. *Adv. Mater.* **2017**, *29* (35), 1701589.
2. Xu, R.; Wu, R.; Shi, Y.; Zhang, J.; Zhang, B. *Nano Energy*. **2016**, *24*, 103-110.
3. Wang, C.; Zhang, P.; Lei, J.; Dong, W.; Wang, J. *Electrochim. Acta.* **2017**, *246*, 712-719.
4. Li, H.; Chen, S.; Lin, H.; Xu, X.; Yang, H.; Song, L.; Wang, X. *Small.* **2017**, *13* (37), 1701487.
5. Sun, Y.; Xu, K.; Wei, Z.; Li, H.; Zhang, T.; Li, X.; Cai, W.; Ma, J.; Fan, H. J.; Li, Y. *Adv. Mater.* **2018**, *30* (35), 1802121.
6. Wu, H.; Lu, X.; Zheng, G.; Ho, G. W. *Adv. Energy Mater.* **2018**, *8* (14), 1702704.
7. Tang, C.; Cheng, N.; Pu, Z.; Xing, W.; Sun, X. *Angew. Chem. Int. Ed.* **2015**, *54* (32), 9351-5.
8. Stern, L.-A.; Feng, L.; Song, F.; Hu, X. *Sci.* **2015**, *8* (8), 2347-2351.
9. Chen, G.-F.; Ma, T. Y.; Liu, Z.-Q.; Li, N.; Su, Y.-Z.; Davey, K.; Qiao, S.-Z. *Adv. Funct. Mater.* **2016**, *26* (19), 3314-3323.
10. Chen, Y.; Ren, Z.; Fu, H.; Zhang, X.; Tian, G.; Fu, H. NiSe-Ni<sub>0.85</sub>Se Heterostructure Nanoflake Arrays on Carbon Paper as Efficient Electrocatalysts for Overall Water Splitting. *Small.* **2018**, *14* (25), 1800763.
11. Wang, X.; Li, W.; Xiong, D.; Petrovykh, D. Y.; Liu, L. *Adv. Funct. Mater.* **2016**, *26* (23), 4067-4077.
12. Liu, Q.; Tang, C.; Lu, S.; Zou, Z.; Gu, S.; Zhang, Y.; Li, C. M. *Chem. Comm.* **2018**, *54* (87), 12408-12411.
13. Dinh, K. N.; Sun, X.; Dai, Z.; Zheng, Y.; Zheng, P.; Yang, J.; Xu, J.; Wang, Z.; Yan, Q. *Nano Energy.* **2018**, *54*, 82-90.
14. Hou, Y.; Qiu, M.; Nam, G.; Kim, M. G.; Zhang, T.; Liu, K.; Zhuang, X.; Cho, J.; Yuan, C.; Feng, X. *Nano Lett.* **2017**, *17* (7), 4202-4209.
15. Zheng, Y. R.; Wu, P.; Gao, M. R.; Zhang, X. L.; Gao, F. Y.; Ju, H. X.; Wu, R.; Gao, Q.; You, R.; Huang, W. X.; Liu, S. J.; Hu, S. W.; Zhu, J.; Li, Z.; Yu, S. H. *Nat. Commun.* **2018**, *9* (1), 2533.
16. Wu, Y.; Liu, Y.; Li, G.-D.; Zou, X.; Lian, X.; Wang, D.; Sun, L.; Asefa, T.; Zou, X. *Nano Energy.* **2017**, *35*, 161-170.
17. Xing, J.; Li, Y.; Guo, S.; Jin, T.; Li, H.; Wang, Y.; Jiao, L. *Electrochim. Acta.* **2019**, *298*, 305-312.
18. Ren, H.; Yu, L.; Yang, L.; Huang, Z.; Kang, F.; Lv, R. *J. Energy Chem.* **2021**, *60*, 194-201.
19. Li, X.; Zhang, L.; Huang, M.; Wang, S.; Li, X.; Zhu, H. *J. Mater. Chem. A.* **2016**, *4*, 14789.
20. Liu, T.; Asiri, A. M.; Sun, X. *Nanoscale.* **2016**, *8*, 3911-3915.
21. Kwak, I. H.; Im, H. S.; Jang, D. M.; Kim, Y. W.; Park, K.; Lim, Y. R.; Cha, E. H.; Park, J. *ACS Appl. Mater. Interfaces.* **2016**, *8*, 5327-5334.
22. Zou, Z.; Wang, X.; Huang, J.; Wu, Z.; Gao, F. *J. Mater. Chem. A.* **2019**, *7*, 2233-2241.